J Mater Sci: Mater Electron (2015) 26:2175–2180
DOI 10.1007/s10854-015-2664-5

# Investigation on the effect of Sn grain number and orientation on the low cycle fatigue deformation behavior of SnAgCu/Cu solder joints

**Ruiting Gao · Xiaoyan Li · Yongxin Zhu**

Received: 24 October 2014 / Accepted: 2 January 2015 / Published online: 7 January 2015


**Abstract** Generally, lead-free solder joints in electronic device are near single or multi crystalline rather than poly crystalline, and the fatigue failure behavior of solder joints is greatly influenced by the solder joint thickness. In this study, the grain number and orientation of solder joints with four solder thicknesses (0.1, 0.2, 0.3, 0.6 mm) were analyzed and the effect of that on the low cycle fatigue deformation behavior of solder joint was also investigated. The orientation analysis was conducted by means of electron backscatter diffraction and the fatigue test was performed under room temperature with a fixed frequency of 1 Hz. Moreover, the deformation evolution on side surface of solder joint was observed by utilizing scanning electron microscope. It is shown that there is no preferred solidification orientation for lead-free solder joints. However, grains in one joint seem to have a similar orientation when the solder thickness is <0.3 mm. Solder joint grain number increases with solder thickness. Besides, the slip direction and slip band density are different for grains with different orientations. Consequently, the deformation on both sides of the grain boundary is inhomogeneous and the fatigue crack is prone to initiate and propagate in this area.

## 1 Introduction

Lead-based solders are replaced by lead-free solders due to environmental concerns and international trade restrictions which ask the eradication of lead from all electronic components by 2006 [1]. Sn–Ag–Cu solder alloys have been widely used as the electronics industry standard lead-free solder [2]. Paralleled with the trend of miniaturization, high packaging density and high reliability for electronic product, lead-free solder joints play an increasingly significant role in mechanical support and electrical connections [3].

As is known to all, solder joint reliability depends on its mechanical and physical property, such as fatigue resistance, hardness, coefficient of thermal expansion (CTE) and so on. Generally, the mechanical property of solder joint is influenced by the microstructure, such as the tin grain number and orientation; distribution and morphology of inter metallic compounds (IMC). Polarized light microscopy (PLM) and electron backscatter diffraction (EBSD) have been widely used to quantify the number of β-Sn grains and to examine the β-Sn crystallographic orientation in solder joints. Telang [4, 5] indicated that the tin-based solder joints are often near single or multi crystalline rather than poly crystalline, and there is no preferred solidification orientation. Yang [6–8] investigated the β-Sn grain number and crystal orientation of SnAgCu/Cu solder joints with of different sizes and found that the SnAgCu/Cu solder joints with different sizes contain only several β-Sn grains and most solder joints were comprised of no more than three Sn grains, and the grain number, crystal orientation and misorientation were independent of solder joint size. However, other researchers advocated that the size reduction of solder joint means the solder changes from poly crystalline to multi crystalline or even single crystalline [9–12], which makes the grain boundaries play a more important role in reliability of electronic package.

From the present work described above, it should be mentioned that the effect of grain number and orientation on solder joints with different sizes is still unclear.

R. Gao (✉) · X. Li · Y. Zhu
School of Materials Science and Engineering, Beijing University of Technology, 100 Ping Le Yuan, Chaoyang District, Beijing 100024, PR China
e-mail: gao_ruiting@163.com

Moreover, its influence on fatigue deformation behavior of solder joint has not been reported, yet. Hence, in this study, the grain number and orientation for solder joints with different solder thickness and its effect on fatigue deformation behavior were investigated.

## 2 Experimental procedure

A single shear-lap joint specimen with copper substrates was designed in this research in order to mimic the shear stress condition experienced by the actual solder joint, as shown in Fig. 1. 96.5Sn–3.0Ag–0.5Cu solder with different thickness (0.1, 0.2, 0.3, 0.6 mm) was used in this study and the substrate metal is selected as copper. The fabrication process of solder joints is as follows: first, in order to remove the oxide layer, the copper substrates were cleaned using the nitric acid solution for 15 s. Second, the solder paste was dispersed on the end of the copper substrate. Then, the copper with solder paste, solder sheet and the other copper substrate were placed in an aluminum fixture orderly. The aluminum fixture was illustrated as Fig. 2. At last, the fixture was put into a reflow oven for 8 min, and the thermal reflow profile was shown in Fig. 3. The specimens should be placed in air for more than 2 weeks in order to relieve the residual stress.

The side surface of the specimens was firstly grinded with 1,500 and 2,000 grit SiC abrasive paper, and then carefully polished with 0.3 μm $Al_2O_3$ and 0.04 μm silica polishing suspension for EBSD and damage evolution observation.

From the EBSD test, the orientation imaging microscopy (OIM) of side morphology could be obtained. Then, low-cycle fatigue test were conducted using a micro-uniaxial fatigue testing system. All fatigue tests were displacement controlled. A triangular waveform was employed, corresponding to the strain ratio R = 0. Displacement amplitude is 50 μm and the frequency is 1 Hz. For the yield stress of copper is far higher than that of the solder, so it is supposed that the deformation was concentrated in the solder. Fatigue tests were terminated when the maximum load drop 20 and 50 %, respectively. Then, deformation evolution was observed from the fine-polished side surface of the solder joint using scanning electron microscope (SEM).

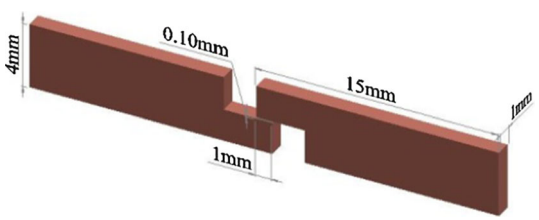


**Fig. 1** Schematic of fabrication of shear-lap solder joint specimen

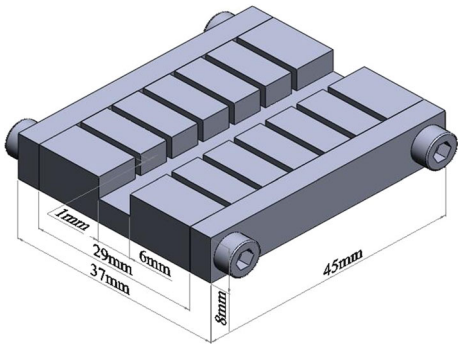


**Fig. 2** Schematic diagram of the aluminum fixture

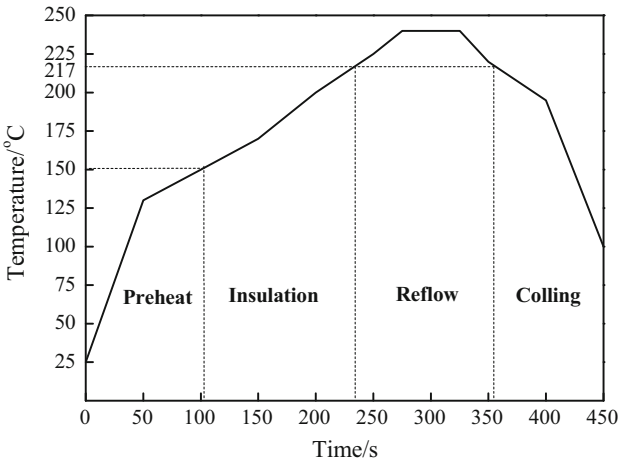


**Fig. 3** The temperature curve of reflow soldering

## 3 Results and discussion

### 3.1 Comparing grains from different thickness solder joints

OIM was widely used to examine the microstructure on the side surface of the solder joints with different thicknesses [13]. The volume fraction of β-Sn makes up the largest part of the 96.5Sn–3.0Ag–0.5Cu solder joint, accordingly, $Cu_6Sn_5$ and $Ag_3Sn$ formed small, needle or disc-shaped particles, which take a low volume fraction of solder joint and they are hardly scanned by OIM. Telang and Bieler [4] found that the OIM maps from two opposite sides of a solder joint show the same crystal orientation, which means that grain on one side throughout the joint, and surface OIM scans are probably representative of the interior of the joint. Therefore, only one side surface OIM scans were taken to determine the distribution of grains in the solder

joints. Figure 4 was OIM maps for solder joint with different solder thickness and different color represents distinct grains. As shown in Fig. 4a–d, only one grain can be scanned in the 0.1 mm thickness solder joint (Fig. 4a), and there are three grains in the 0.2 and 0.3 mm thickness solder joints (Fig. 4b, c). Furthermore, six grains were observed in the 0.6 mm thickness solder joint (Fig. 4d). So it can be concluded that solder joints grain number increase with enlarging solder thickness.

Based on the OIM analysis, the three-dimensional orientation figures were obtained by the HKL-EBSD Simulator, all of the crystal orientations in each joint were illustrated in Fig. 4e–h. The β-Sn crystal shows the body-centered tetragonal structure, and the lattice constant are a = b = 5.8326, c = 3.1821, respectively. The blue axis in Fig. 4e–f represents the c axis, and the red and green represent a and b axis, respectively. The details about the orientations of each grain in different thicknesses solder joints were shown in Table 1. There is one-to-one correspondence between the Euler angles and Miller indices of each grain. As shown in Fig. 4f, there was very small misorientation between the neighbor grains for 0.2 mm thickness solder joint. However, the grain number increased and orientation become disordered with increasing the solder thickness, as shown in Fig. 4h. It can be explained by the growth of additional nucleation

**Table 1** The orientation of each grain in different thickness solder joint

| Solder thickness/mm | Euler angle/° | | | Miller indices |
|---|---|---|---|---|
| | $\varphi_1$ | $\Phi$ | $\varphi_2$ | |
| 0.1 mm | 17.1 | 105.6 | 25.0 | (3 6 −1) [5 −2 3] |
| 0.2 mm | 72.4 | 167.5 | 5.3 | (0 1 −2) [1 2 1] |
| | 119.4 | 169.2 | 46.4 | (1 1 −4) [1 3 1] |
| | 77.1 | 160.4 | 11.2 | (1 5 −8) [2 4 3] |
| 0.3 mm | 41.4 | 113.0 | 64.6 | (4 2 −1) [1 −1 2] |
| | 33.7 | 120.7 | 44.4 | (2 2 −1) [2 −1 2] |
| | 56.6 | 121.7 | 43.9 | (2 2 −1) [1 0 2] |
| 0.6 mm | 92.4 | 119.8 | 5.3 | (0 3 −1) [0 1 3] |
| | 93.5 | 116.6 | 88.8 | (4 0 −1) [1 0 4] |
| | 151.6 | 99.4 | 24.9 | (1 2 0) [−2 1 2] |
| | 35.2 | 103.3 | 66.9 | (7 3 −1) [2 −3 5] |
| | 31.2 | 100.3 | 63.0 | (9 5 −1) [2 −3 4] |
| | 152.5 | 102.8 | 25.7 | (3 7 −1) [−3 2 3] |

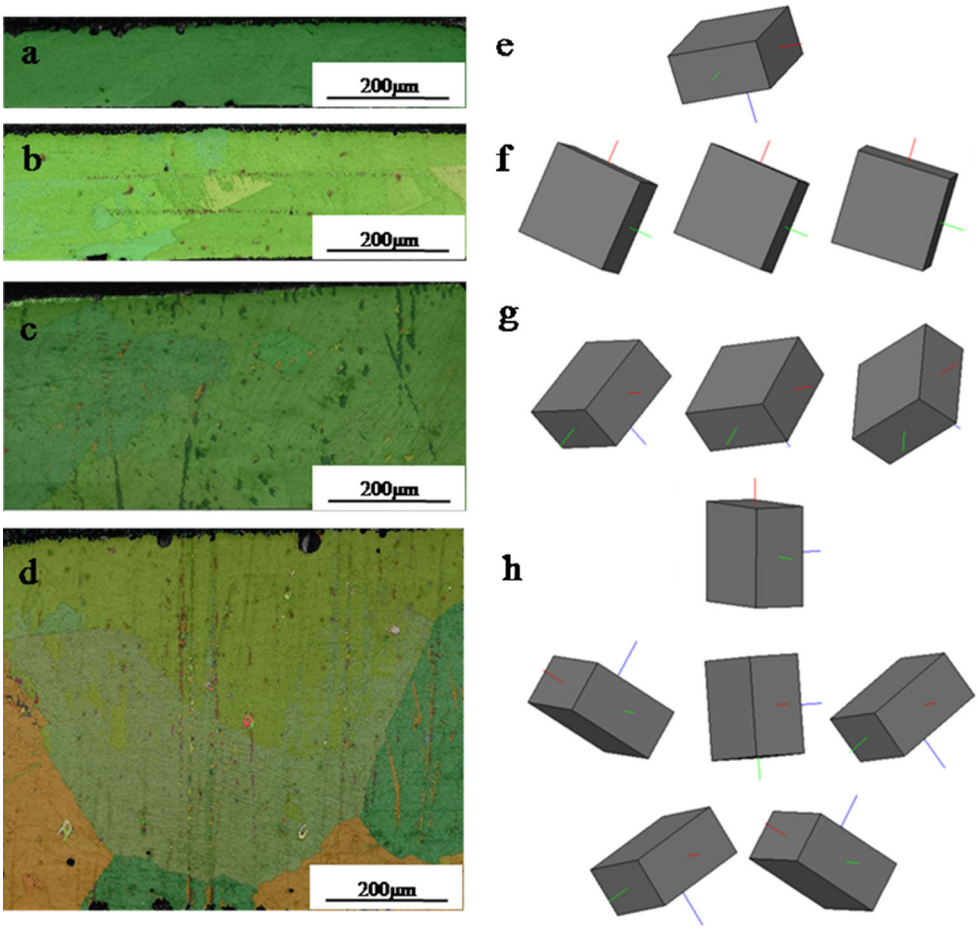


**Fig. 4** The OIM maps of different thickness solder joints (0.1, 0.2, 0.3 and 0.6 mm) and corresponding three-dimensional orientation figures

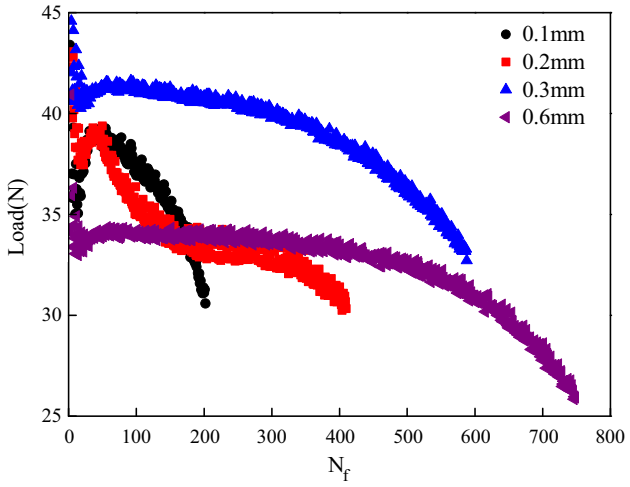


**Fig. 5** Maximum load drop 20 % during the cycles

centers. In general, the solder joints solidified as single crystalline or multi crystalline, and during the process of cooling, coherent β-Sn formed easier. Investigations of four group specimens indicated that there is no preferred solidification orientation for lead-free solder joints. Meanwhile, tiny IMC had little influence on the process of grain growth.

### 3.2 Low cycle fatigue deformation

Generally, the maximum load drop of every cycle indicates the crack initiation and propagation process in solder joint. Hence, the fatigue resistance ability is determined by the load drop rate. In order to observe the deformation evolution on solder joint side surface, fatigue test stopped when the maximum load of every cycle drops 20 %. Figure 5 is the corresponding maximum load drop curves.

OIM map for solder joint with 0.3 mm thickness and corresponding surface morphologies scanned by SEM are shown in Fig. 6. Figure 6a shows the low power field Euler angle color of whole region for 0.3 mm thickness joint, the inverse pole figure of Fig. 6b shows the normal *y* direction of joint distribution in a-b-c coordinate system. The scanning step is selected as 1.5 μm to acquire adequate details. Figure 6c shows the initial state by OIM map from the surface of joint, and Fig. 6d shows the change after maximum load drop 20 % fatigue test. In this joint only two colors can be seen, the color on the top left corner is

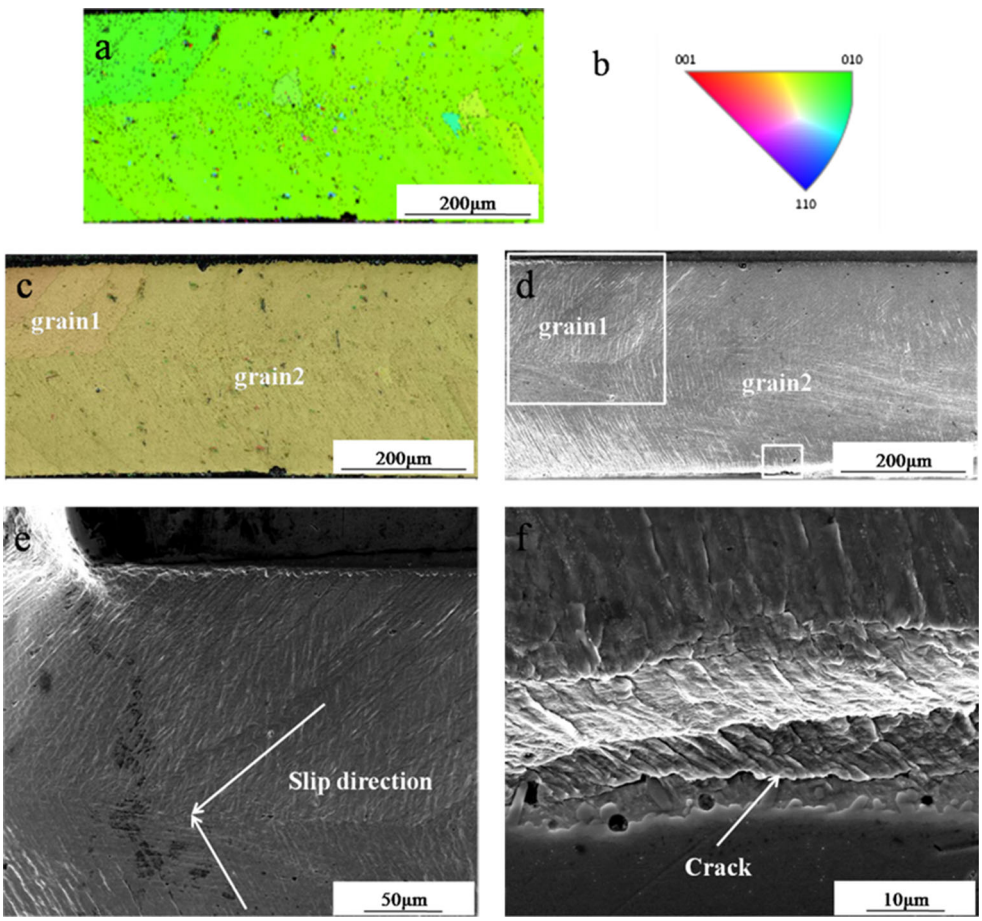


**Fig. 6** Damage evolution when maximum load drop 20 % in 0.3 mm thickness solder joint

different from other part of the joint, which represent two orientation grains, named grain1 and grain2. Based on the OIM map analysis, the Miller indices of grain1 is (30-2) [021] and grain2 is (21-1) [011]. As shown in Fig. 6d, the slip direction on grain1 is different from other part of the joint, the boundary hampered the process of the slip and then the grain boundary obviously can be seen. Enlarging the area of grain1, details of the deformation morphology is shown in Fig. 6e. Slip directions on both sides of grain boundary are nearly vertically. Besides, the density of slip band on grain1 is slightly larger than that under the grain boundary. The deformation characteristics are closely related to the orientation of each grain, it was suggested that one main slip system in each grain would be activated during the deforming process. The {010} <100> slip system would be activated first in the single crystal β-Sn under room temperature [9]. Figure 6f shows the details about the small box region in Fig. 6d. It is significant that slip band accumulated near the IMC layer, which is caused by the restraint effect of substrate metal. Consequently, crack initiated here due to the inhomogeneous deformation.

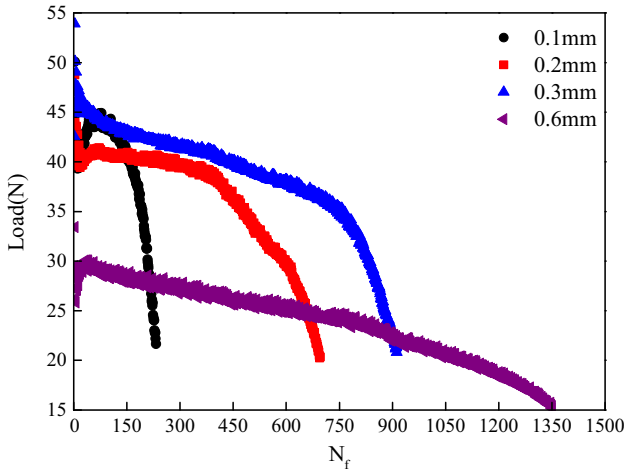


**Fig. 7** Maximum load drop 20 % during the cycles

Many studies define the cyclic number of maximum load drop 50 % as the fatigue life of the solder joint [14]. It means that the crack has started to propagate and the solder joint is near failure at the point of 50 % load drop. In order to observe the failure of the solder joint, fatigue test stopped when the maximum load of every cycle drops 50 %. Figure 7 is the corresponding maximum load drop curves. Figure 8 are OIM map for solder joint with 0.6 mm thickness and corresponding surface morphologies scanned

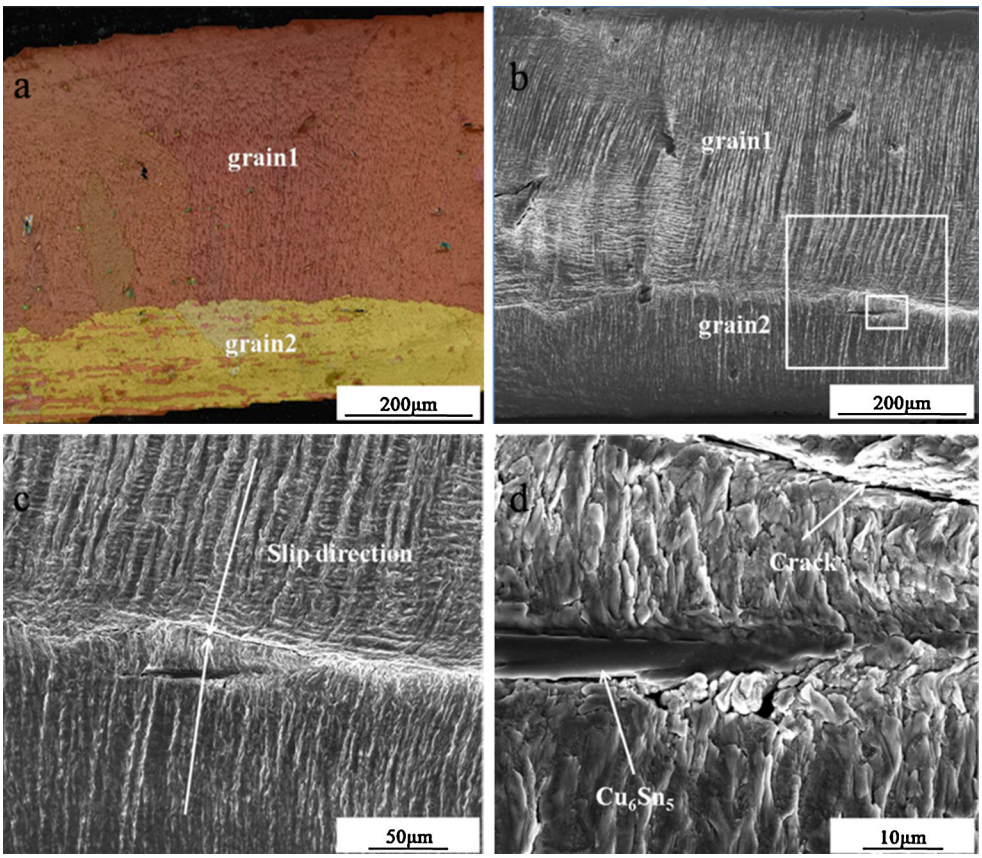


**Fig. 8** Damage evolution when maximum load drop 50 % in 0.6 mm thickness solder joint

by SEM. As shown in Fig. 8a, it is noticeable that the grain boundary throughout the whole joint and two dominating grains occupying most of the 0.6 mm thickness as-reflowed solder joint. Based on the OIM map analysis, the orientation of each grain has a big difference, the Miller indices of the red one which named grain1 is (122) [−1 −1 2] and the yellow one which named grain2 is (111) [−1 −2 4]. Some studies suggested that samples with <112> axis have higher stacking fault energy and easily cause cross-slip, so that the slip deformation appears corrugate slip band and it occurs more easily than other samples with different orientations. After fatigue test with 50 % maximum load drop, the identical surface of solder joint was observed by SEM timely. As shown in Fig. 8b, the slip process occurred incrementally with each cycle, and the deformation is more severe than that after fatigue test with 20 % maximum load drop. Meanwhile, inhomogeneous deformation occurred near the grain boundary, the density of slip band has a large difference between the two grains, in spite of similar slip direction evidenced in Fig. 8c, a mass of deformation occurred in the grain with [−1 −1 2] axis. As shown in Fig. 8d, crack on the top right corner propagated along the grain boundary and the fatigue failure will occur real soon. Besides, crack was initiated around the $Cu_6Sn_5$ phase, but it was not further propagated, which shows it has little effect on the fatigue property of solder joint. On the other hand, restraint effect is decreased with increasing the solder thickness, so that there is less deformation on the interface near the copper substrate.

## 4 Conclusions

1. The grain number of solder joints increases with solders thickness. The solder joint studied in this research is a single or multi crystalline rather than poly crystalline.
2. Grains for solder joint with thickness <0.3 mm have similar orientations. With increasing the thickness, especially the thickness over 0.3 mm, the orientations difference of each grain appears markedly increase.
3. Only one or two slip systems start during the fatigue deformation process of β-Sn single crystalline, so that under low cycle fatigue test there is a large difference in the slip direction and slip band density among the grains with different orientations. Inhomogeneous deformation made the fatigue crack initiation and propagated along the grain boundaries.

**Acknowledgments** This study was financially supported by National Natural Science Foundation of China (No. 51275007) and Key Project of Beijing Educational Committee Scientific Research Plan (No. KZ201410005009), which were acknowledged.

## References

1. A.U. Telang, T.R. Bieler, A. Zamri, F. Pourboghrat, Acta Mater. **55**, 2265–2277 (2007)
2. W.W. Lee, L.T. Nguyen, G.S. Selvaduray, Microelectron. Reliab. **40**, 231–244 (2000)
3. H. Rhee, K.N. Subramanian, Solder. Surf. Mt. Technol. **18**(1), 19–28 (2006)
4. A.U. Telang, T.R. Bieler, Scr. Mater. **52**, 1027–1031 (2005)
5. A.U. Telang, T.R. Bieler, JOM **6**, 44–49 (2005)
6. P. Zimprich, U. Saeed, A. Betzwar-Kotas, B. Weiss, H. Ipser, J. Electron. Mater. **37**(1), 102–109 (2008)
7. M. Sona, K.N. Prabhu, J. Mater. Sci. Mater. Electron. **24**, 3149–3169 (2013)
8. S.H. Yang, Y.H. Tian, C.Q. Wang, J. Mater. Sci. Mater. Electron. **21**, 1174–1180 (2010)
9. J.T. Liu, Z.G. Wang, J.K. Shang, Acta Metall. Sin. **44**(12), 1409–1414 (2008)
10. J. Zhao, Y. Mutoh, Y. Miyashita, S.L. Mannan, J. Electron. Mater. **31**(8), 879–886 (2002)
11. H. Conrad, Z. Guo, Y. Fahmy, D. Yang, J. Electron. Mater. **28**(9), 1062–1070 (1999)
12. L.M. Yin, X.P. Zhang, C.S. Lu, J. Electron. Mater. **38**(10), 2179–2183 (2009)
13. P. Yang, Electron backscatter diffraction technology and its applications (Beijing, 2007), pp. 141–157
14. D. Shangguan, *Lead-free solder interconnect reliability* (ASM international, Geauga, 2005), pp. 84–128